Kinetics and Mechanism of Chromium(VI) Reduction to Chromium(III) by L-Cysteine in Neutral Aqueous Solutions

Peter A. Lay* and Aviva Levina

School of Chemistry, University of Sydney, New South Wales 2006, Australia

Received June 5, 1996[⊗]

The reduction of chromate by a 50−250-fold excess of L-cysteine (pH = 7.0−7.7; self-buffered; [$NaClO_4$] = 0−1 M; T = 288−308 K) was studied by global analysis of kinetic data sets in coordinates of absorbance−wavelength (230−640 nm)−time. The observed changes were fitted by a sequence of three pseudo-first-order processes. The main Cr(III) product (≥95%) was identified as *N*(*cis*),*O*(*cis*),*S*(*trans*)-bis(L-cysteinato(2−))-chromate(III) on the basis of its UV−visible and CD spectra. The chemical natures of the intermediates and the reaction mechanism were proposed on the basis of (i) observed rate constant dependences on the reaction conditions ($k_1^{obs} = 0.19 + 35[RS^-]$ s^{-1}; $k_2^{obs} = 30\ [RSH]^2/(1 + 20[RSH])$ s^{-1}; $k_3^{obs} = 0.04$ s^{-1} at μ = 1 M and T = 298.1 K), where [RS^-] and [RSH] are the concentrations of deprotonated and protonated forms of L-cysteine); (ii) estimated spectra of intermediates and their dependences on the reaction conditions; and (iii) comparison of kinetic features of the studied reaction and the related processes (Cr(V) + L-cysteine; Cr(VI) + 2-mercaptoethylamine; Cr(VI) + 3-mercaptopropionic acid). The proposed mechanism includes the following: (i) formation of a Cr(VI) complex with two cysteine ligands; (ii) its conversion to a precursor Cr(III) complex by sequential one-electron reductions with three cysteine molecules; and (iii) intramolecular rearrangement of the precursor Cr(III) complex leading to the final product. Possible implications of the kinetic data to the studies of Cr(VI) genotoxicity mechanisms are discussed.

Introduction

The mechanism of Cr(VI) reduction to Cr(III) by the tripeptide glutathione (γ-Glu-Cys-Gly, GSH) in neutral aqueous media has been the subject of extensive studies.[1] The intermediates formed in this reaction (Cr(V) and Cr(IV) complexes and thyil radicals) have been proposed to be involved in the genotoxicity of Cr(VI).[2] Although the redox activity of GSH under physiological conditions is connected exclusively with the SH group of the Cys fragment, a number of other donor groups present in the GSH molecule can potentially lead to the formation of a variety of complexes with different redox states of Cr during the reaction.[3−5] Therefore, the reduction mechanism can be expected to be quite complex.

The reaction of Cr(VI) with L-cysteine in neutral media has been studied as a simpler model for the Cr(VI) + GSH redox reaction.[6−8] The most detailed investigation of Kwong and Pennington[6] led to a proposed mechanism (Scheme 1), which includes the initial formation of a Cr(VI)−Cys adduct, followed by its two-electron reduction by a second Cys molecule with the formation of a Cr(IV) intermediate. The mechanism of the following stages, leading to a Cr(III) cysteinato complex, is uncertain. Some limitations of the published data[6−8] should be mentioned: (i) the kinetic studies did not include variations in pH; (ii) various buffers (acetate, Tris, HEPES) were used for maintaining constant pH; however, the influence of the nature and concentration of buffer to the Cr(VI) + Cys reaction was not studied; and (iii) all kinetic studies were performed by following the decrease of absorbance at 370 nm, which was identified with a decrease of the Cr(VI) concentration. The spectral changes at other wavelengths were not studied.

Scheme 1. Proposed Mechanism for the Cr(VI) Reaction with Cys in Neutral Media (Data of Kwong and Pennington)[6]

$$HCrO_4^- + \text{L-CysSH} \rightleftharpoons \text{L-CysS}CrO_3^- + H_2O$$

$$\text{L-CysS}CrO_3^- + \text{L-CysSH} \longrightarrow \text{L-cystine} + HCrO_3^-$$

$$HCrO_4^- + HCrO_3^- + 8\text{L-CysSH} \longrightarrow 2Cr(\text{L-Cys-N,O,S})_2^- + 2\text{L-cystine} + 7H_2O$$

The development of mathematical methods for simultaneously processing a large series of time-dependent spectra, i.e., global analysis and singular value decomposition (SVD),[9] have led to more extensive and rigorous UV−visible spectroscopy-based kinetic studies. Indeed, three-dimensional sets of data (absorbance−wavelength−time) instead of two-dimensional ones (absorbance at single wavelength−time) can now be fitted by kinetic models. Model-independent determination of the number of spectrally different components existing in the reaction mixture, and the estimation of spectra for short-lived intermediates, are the additional possibilities of this new technique. Some successful applications of the above-described approach to kinetic and mechanistic studies have been recently reported.[10]

⊗ Abstract published in *Advance ACS Abstracts,* November 15, 1996.

(1) Cieślak-Golonka, M. *Polyhedron* **1996**, *15*, 3667−3689 and references therein.
(2) O'Brien, P.; Kortenkamp, A. *Transition Met. Chem.* **1995**, *20*, 636−642 and references therein.
(3) Brauer, S. L.; Wetterhahn, K. E. *J. Am. Chem. Soc.* **1991**, *113*, 3001−3007.
(4) O'Brien, P.; Pratt, J.; Swanson, F. J.; Thornton, P.; Wang, G. *Inorg. Chim. Acta* **1990**, *169*, 265−269.
(5) Abdullah, M.; Barrett, J., O'Brien, P. *J. Chem. Soc., Dalton Trans.* **1985**, 2085−2089.
(6) Kwong, D. W. J.; Pennington, D. E. *Inorg. Chem.* **1984**, *23*, 2528−2532.
(7) Connett, P. H.; Wetterhahn, K. E. *J. Am. Chem. Soc.* **1985**, *107*, 4282−4288.
(8) O'Brien, P.; Wang, G.; Wyatt, P. B. *Polyhedron* **1992**, *11*, 3211−3216.
(9) (a) Maeder, M.; Zuberbuhler, A. D. *Anal. Chem.* **1990**, *62*, 2220−2224. (b) Beechem, J. M. *Methods Enzymol.* **1992**, *210*, 37−55. (c) Henry, E. R.; Hofrichter, J. *Methods Enzymol.* **1992**, *210*, 129−192.

S0020-1669(96)00663-5 CCC: $12.00

Table 1. Conditions of the Kinetic Experiments

parameter	conditions I	conditions II
spectrophotometer	SX-17MV	HP 8452A
wavelength interval, nm	360−640	230−400
pathlength, cm	0.2	1.0
$[Cr(VI)]_0$, mM	0.5−1.5	0.015−0.075
$[Cys]_0$, mM	50−250	2.0−15
pH	7.0−7.7[a]	7.1−7.6[a]
$[NaClO_4]$, M	0−1	0.10
T, K	287.5−308.4	298.1
reaction time, s	100−200	1800

[a] $[NaOH]_0 = (0.025-0.15)[Cys]_0$. Typically, the pH increased during the process by 0.01−0.03 unit at $[Cys]_0 = 100-250$ mM, by 0.03−0.07 unit at $[Cys]_0 = 50-100$ mM, and by 0.05−0.1 unit at $[Cys]_0 = 2.0-15$ mM.

In the current work, we have applied global analysis and SVD for detailed kinetic studies of the Cr(VI) reaction with L-cysteine in neutral aqueous solutions. The reasons for such a choice are the following: (i) this reaction is important for the studies of Cr(VI) biological activity (see above); (ii) Cys is a good buffer at pH ∼ 7, so no additional buffers are required; and (iii) the chemistry of possible products (Cr(III)−Cys complexes) is relatively well established.[11−13]

Experimental Section

Caution. *Cr(VI) compounds are human carcinogens,*[14] *and Cr(V) complexes are mutagenic and potentially carcinogenic.*[2] *Contact with skin and inhalation must be avoided.*

Reagents. L-Cysteine, L-cystine (designated as Cys-Cys in the following text), 2-mercaptoethylamine hydrochloride, 3-mercaptopropionic acid (all AR grade, Sigma), $Na_2CrO_4 \cdot 4H_2O$, $Cr(NO_3)_3 \cdot 9H_2O$, NaOH, $NaClO_4$, and ethylenediamintetraacetic acid disodium salt (Na_2EDTAH_2) (all p.a. Merck) were used as received. Sodium *N*(*cis*),*O*(*cis*),*S*(*trans*)-bis(L-cysteinato(2−))chromate(III) dihydrate (designated as $[Cr(Cys)_2]^-$ in the following text) and sodium bis(2-ethyl-2-hydroxybutanoato(2−))oxochromate(V) monohydrate (designated as $[CrO(ehba)_2]^-$) complexes were synthesized accordingly to published procedures.[11,15] MilliQ water (purified by predistillation, filtration through active carbon and ion exchangers, followed by reversed osmosis) was used for preparation of the solutions.

Methods and Equipment. An Applied Photophysics SX-17MV stopped-flow spectrophotometer (dead time ∼2 ms), equipped with Acorn A5000 computer, was used for kinetic studies of relatively fast processes (conditions I in Table 1). A quartz optical cell with $l = 0.2$ cm was used, and the stopped volume was 200 μL. Freshly prepared solutions of Cr(VI) and Cys in the appropriate media were mixed in 1:1 ratio. All the stopped-flow kinetic measurements, unless specially noted, were performed under an Ar atmosphere using the SX-17MV anaerobic accessory to minimize the possible influence of O_2. Solutions were saturated with Ar immediately before use. Residual $[O_2]$ in the reaction medium was <0.05 mM at 25 °C (measured by YSI-58 dissolved oxygen meter). Thus, the influence of O_2 is assumed to be negligible. A Grant LTD 6-G thermostated water bath was used for maintaining a constant temperature (±0.1 °C) within the optical cell and the syringes. The reaction system was thermostated (for 15 min) after every refill of the syringes.

A HP 8452A diode-array spectrophotometer (resolution 2 nm) equipped with a temperature control unit (±0.1 °C) was used for studies of slower reactions (conditions II in Table 1). For conditions II, the freshly prepared, deoxygenated (by bubbling of Ar for 15 min) and thermostated solutions of Cys and Cr(VI) were mixed manually in 1-cm quartz cell, stoppered by a Teflon cap. Time-dependent spectra were acquired every 60 s (integration time 1 s). Steady-state UV−visible spectra were also recorded on the HP 8452A spectrophotometer using a 1-cm quartz cell. Circular dichroism (CD) spectra were recorded on Jasco 710 spectropolarimeter (resolution 1 nm, 20 °C, 1-cm quartz cell). An Activon 210 ionometer with AEP 321 glass−calomel electrode was used for pH measurements.

Choosing Conditions for Kinetic Experiments. Most of the kinetic data were collected by multiwavelength stopped-flow technique at 360−640 nm (conditions I in Table 1). The useful wavelength interval is restricted by the strong absorbance of Cys in the UV region[16] and by limitations of the SX-17MV monochromator in the near-IR region. As both Cys and Cys-Cys are colorless in the above-mentioned interval, water was used as the absorbance reference. However, as the absorbance with $\lambda_{max} \sim 260$ nm is specific for Cr(III)−S bond,[12,13] observation of spectral changes in this region is very important for mechanistic studies of the Cr(VI) + Cys reaction. This becomes possible at lower initial concentrations of reagents (conditions II in Table 1). The reactions at these conditions are too slow for the stopped-flow method. Therefore, the time-dependent spectra were followed using the diode-array spectrophotometer. For these experiments, the absorbance of initial solutions, containing Cys, NaOH, and $NaClO_4$, was used as a reference. The difference between the two methods should be emphasized. The former produces kinetic curves (each consisting, typically, from 1000 points in logarithmic time base) at certain wavelengths (in this study, every 10 nm in 360−640-nm interval). The latter produces spectra (with a 2-nm resolution) for certain time points (typically, 30 points every 1 min). Obviously, the first method allows more accurate kinetic analysis (especially for the initial stages of reaction).

Processing of Kinetic Data. A nonlinear least-squares program for fitting separate kinetic curves was available from the SX-17MV software. Global analysis (Glint)[17] software was used for multivariate analyses of the kinetic data obtained with both SX-17MV and HP 8452A spectrophotometers. For conditions II (Table 1), all data points were used for global analysis. For conditions I (overall reaction time 100−200 s), the absorbance changes due to the chemical reactions at the first ∼0.25 s were negligible. However, in many experiments, small sudden changes of absorbance happened in this time. These artifacts were connected with the small posttrigger flow through the photometric cell[18] and could lead to incorrect conclusions from the SVD analyses. Therefore, the data corresponding to the first ∼0.25 s of the reaction (350 points in logarithmic time base) were ignored. For the fast processes (Cr(V) + Cys; reaction time ≤10 s), no significant artifacts on the kinetic curves were observed. Therefore, in these cases only the data points corresponding to dead time (first 2 ms) were ignored. Application of the SVD procedure (within the Glint software) to the resulting data matrices allowed a separation of significant spectral changes from the noise and monitoring of changes in the number of independent absorbing species during the reaction. On the basis of these observations, the simplest kinetic models were proposed. These models were then fitted to the matrices of experimental data using the Marquardt−Levenberg optimization procedure within the Glint software package. This procedure provided the optimal values of rate constants (k_i), as well as the corresponding concentration plots and estimated spectra of the intermediates. The quality of the fit was determined from the differences between estimated and experimental values of absorbance (matrix of residuals). Further processing of global analysis results, such as linear and nonlinear least-squares fits of dependences

(10) For example: (a) Hendler, R. W.; Bose, S. K.; Shrager, R. I. *Biophys. J.* **1993**, *65*, 1307−1317. (b) Stultz, L. K.; Binstead, R. A.; Reynolds, M. S.; Meyer, T. J. *J. Am. Chem. Soc.* **1995**, *117*, 2520−2532.
(11) De Meester, P.; Hodgson, D. J.; Freeman, H. C.; Moore, C. J. *Inorg. Chem.* **1977,** *16*, 1494−1498.
(12) Santos, T. M.; Pedrosa de Jesus, J.; O'Brien, P. *Polyhedron* **1992**, *11*, 1687−1695.
(13) Kaiwar, S. P.; Sreedhara, A.; Raghavan, M. S. S.; Rao, C. P.; Jadhav, V.; Ganesh, K. N. *Polyhedron*, **1996**, *15*, 765−774 and references therein.
(14) International Agency for Research on Cancer (IARC). *IARC Monogr. Eval. Carcinog. Risk Chem. Hum. Suppl.* **1987**, *7*, 165−168.
(15) Krumpolc, M.; Roček J. *J. Am. Chem. Soc.* **1979**, *101*, 3206−3209.
(16) Although the reaction mixture is transparent at $\lambda > 300$ nm under the studied conditions, at $\lambda = 300-360$ nm, the analysis is complicated by absorbance changes due to the formation of Cys-Cys.
(17) King, P. J.; Maeder, M. *Glint−Global Kinetic Analysis. Version 3.31*. Applied Photophysics Ltd., Leatherhead, UK, 1993.
(18) *The Biosequential SX-17MV Stopped-Flow Reaction Analyser. Hardware Manual*. Applied Photophysics Ltd., Leatherhead, UK, 1995.

Scheme 2. Main Protolytic Forms of Cys and the Related Thiols in Neutral Aqueous Media (on the Basis of the Data of Connett and Wetterhahn)[20]

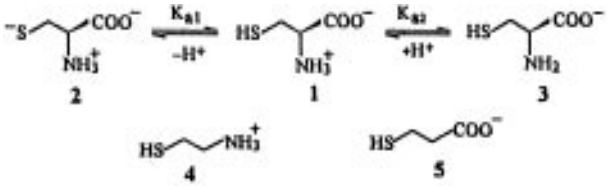

between the observed rate constants and the reaction conditions, as well as the analysis of estimated spectra, was performed using Origin[19] software.

A knowledge of Cys protolytic equilibria was required for the kinetic analysis. Three forms of Cys (**1**−**3** in Scheme 2) were assumed to exist in rapid equilibria under the studied conditions on the basis of acidity data.[20] In the current work, the pH was varied by changing the $[Cys]_0/[NaOH]_0$ ratio and no additional buffers were required. Therefore, the concentrations of protonated and deprotonated forms of Cys were determined by

$$[RSH] = [Cys]_0 - [NaOH]_0 \quad (1)$$

$$[RS^-] = [NaOH]_0 \quad (2)$$

where [RSH] = [**1**] and [RS$^-$] = [**2**] + [**3**] (see Scheme 2). No discrimination between **2** and **3** was made in the kinetic analysis. Indeed, such discrimination would be problematic because of the similar K_a values ($pK_{a1} = 8.40$; $pK_{a2} = 8.85$ at $\mu = 0.5$ M; 298 K).[20]

Additionally, we studied the reactions of Cr(VI) with the compounds related to Cys, 2-mercaptoethylamine and 3-mercaptopropionic acid, which exist in neutral aqueous solutions as the cation **4** and anion **5**, respectively (Scheme 2).[20]

Results

Product Studies. $[Cr(Cys)_2]^-$ has been identified as the sole detectable Cr(III) product[21] of the studied process on the basis of the correspondence between the UV−visible and CD spectra of the reaction mixtures after completion of the Cr(VI) + Cys redox process, and the spectra for authentic $[Cr(Cys)_2]^-$ (Figure 1). The most important evidence for the nature of the product has been obtained from the comparison of spectra in UV region (Figure 1a). The equally intense Cr−S charge transfer bands[12] with $\lambda_{max} \sim 260$ nm and $\epsilon_{max} \sim 10^4$ M^{-1} cm^{-1} have been observed for the complexes obtained from both Cr(III) + Cys and Cr(VI) + Cys reactions, while no such band was observed for the Cr(III) complex with Cys-Cys. Any coordination of Cys-Cys with Cr during the Cr(VI) + Cys reaction would lead to a decrease of product absorbance at ∼260 nm. Thus, these data confirm the assumption[6] that the oxidized form of substrate (Cys-Cys) is not included into the coordination sphere of the Cr(III) product.

Multiwavelength Stopped-Flow Studies (conditions I in Table 1). The main spectral events observed under the studied conditions are as follows: (Figure S1 in Supporting Information): (i) a decay of initial absorbance at 360−400 nm; (ii) a growth and decay of the intermediate absorbance at 410−500 nm; and (iii) a growth of product absorbance at 510−640 nm. The most characteristic kinetic curves (370, 460, and 620 nm) are shown in Figure 2a. Some features of these characteristic curves, not been mentioned in the previous publications,[6−8] were observed. Although the kinetic curves at 370 nm for the reaction of Cr(VI) with Cys have been treated previously as a single first-order decay process,[6,8] deviations from such simple kinetics occur in the initial stage of reaction (a representative example is shown in Figure S2 in Supporting Information). The growth of absorbance at 460 nm occurs more rapidly with an increase in pH, however, the maximal absorbance at 460 nm decreases with an increase in pH (Figure S3 in Supporting Information). The relatively fast growth of absorbance at 620 nm is followed by a slower stage (Figure 2a). While the changes of absorbance at 370 and 460 nm occur only during the first 30 s after the mixing of reagents (under the conditions of Figure 2), the spectral changes at 620 nm continue for more than 100 s.

However, the present kinetic data were analyzed by global analysis rather than using the analysis of separate kinetic curves. Application of the SVD procedure to the global sets of kinetic data (Figure S4 and Table S1 in Supporting Information) gives

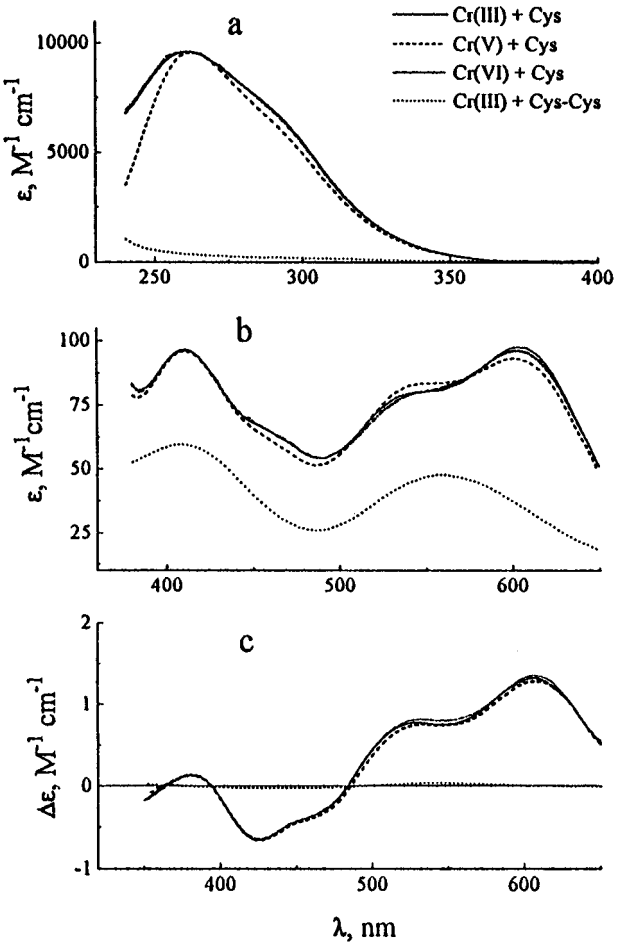

Figure 1. UV (a), visible (b), and CD (c) spectra of Cr(III)/Cys and Cr(III)/Cys-Cys complexes. Conditions for Cr(III) + Cys: 5 mM $Na[Cr(Cys)_2]$ + 200 mM Cys + 20 mM NaOH (pH = 7.3); reaction time 1 h (20 °C). Conditions for Cr(V) + Cys: as for Cr(III) + Cys, using 5 mM $Na[CrO(ehba)_2]$ instead of $Na[Cr(Cys)_2]$. Conditions for Cr(VI) + Cys: as for Cr(III) + Cys, using 5 mM Na_2CrO_4 instead of $Na[Cr(Cys)_2]$. Conditions for Cr(III) + Cys-Cys: 2 mM $Cr(NO_3)_3$ added to 2 mM water solution of Cys-Cys; the mixture boiled for 30 min and then the pH adjusted to 7.3 with NaOH. Spectra of undiluted (b, c) or diluted 50 times with water (a) reaction mixtures were taken. Background solutions were prepared analogously to the analyzed solutions, but without the addition of Cr compounds.

(19) *Origin. Technical graphics and data analysis for Windows, Version 3.5.* Microcal Software Inc., Northampton, USA, 1991−1994.

(20) Connett, P. H., Wetterhahn, K. E. *J. Am. Chem. Soc.* **1986**, *108*, 1842−1847.

(21) Quantitative determination of $[Cr(Cys)_2]^-$ has been performed by its separation on Sephadex A-25 anion-exchange column and following oxidation to Cr(VI) by alkaline H_2O_2 solution.[6] Not less than 95% of Cr(VI) was recovered by this method. The formation of Cys-Cys was shown qualitatively by IR spectroscopy. However, the quantitative determination of Cys-Cys is difficult because of its small concentration relative to unreacted Cys and its possible additional formation by autoxidation of Cys during the analytical procedures.

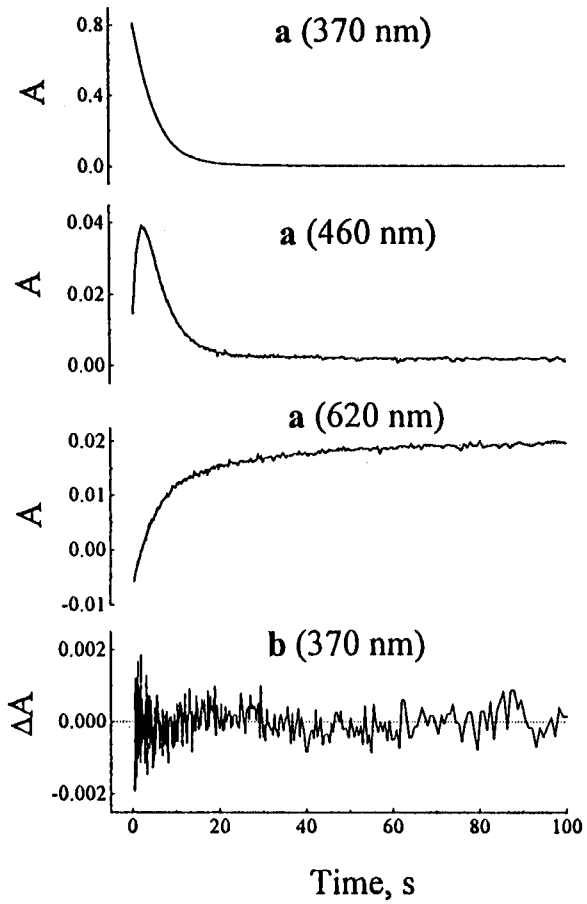

Figure 2. Experimental and estimated kinetic curves (a) and the difference between experimental and estimated absorbance values (b) for the reaction Cr(VI) + Cys. Experimental data (solid lines); estimated from Scheme 3 (dotted lines). Reaction conditions: $[Cr(VI)]_0 = 1$ mM; $[Cys]_0 = 200$ mM; $[NaOH]_0 = 10$ mM (pH = 7.00); $[NaClO_4] = 1$ M; 298.1 K.

Scheme 3. Simplest Kinetic Model for the Reaction Cr(VI) + Cys under Conditions I (Table 1)

$$\mathbf{A} \xrightarrow{k_1^{obs}} \mathbf{B} \xrightarrow{k_2^{obs}} \mathbf{C} \xrightarrow{k_3^{obs}} \mathbf{D}$$

evidence for the sequential appearance of four different absorbing species (including the initial one) in the reaction mixture. Indeed, all of the kinetic data sets were readily described by a sequence of three pseudo-first-order steps (Scheme 3). The optimized values of k_i^{obs} for all kinetic experiments are enumerated in Table S2 (Supporting Information). In all cases, the differences between experimental absorbance values and those estimated from Scheme 3 did not exceed the spectrophotometer noise level (0.001−0.002 AU); a typical example is shown in Figure 2b. In addition, the rate constant data from the global analysis were matched to those from treatment of separate kinetic curves (see Figure 2a): k_1^{obs} corresponds to growth of absorbance at 460 nm, k_2^{obs} to the decay of absorbance at 460 nm and "fast" growth of absorbance at 620 nm, and k_3^{obs} to the "slow" growth of absorbance at 620 nm. Kinetic curves at 370 nm are fitted by a sequence of two processes with rate constants k_1^{obs} and k_2^{obs}.

Over the studied temperature range (288−308 K), the observed rate constants obeyed the Arrhenius law (see the data of Table S2). All stages of the reaction are characterized by large negative $\Delta S^{\ddagger}$ values (Table S3, Supporting Information). Further detailed kinetic studies were limited to 298.1 K.

Table 2. Parameters of Kinetic Eqs 3−5

eq	parameter	**1**[a]	**2**[b]	**3**[c]
3	a_1, s^{-1}	0.19 ± 0.03	0.04 ± 0.01	
	b_1, $M^{-1}\,s^{-1}$	35 ± 2	42 ± 2	
4	a_2, $M^{-2}\,s^{-1}$	30 ± 4[d]	98 ± 12	700 ± 300
	b_2, M^{-1}	20 ± 3[d]	68 ± 9	800 ± 400
5	a_3, s^{-1}	0.04 ± 0.01	0.03 ± 0.01	

[a] Conditions I from Table 1. $[Cys]_0 = 100-250$ mM; $[NaClO_4] = 1$ M; $T = 298.1$ K. [b] Conditions I from Table 1. $[Cys]_0 = 50-150$ mM; $[NaClO_4] = 0.5$ M; $T = 298.1$ K. [c] Conditions II from Table 1. [d] Equal values were found for two series of experiments: $[Cys]_0 = 100-250$ mM at pH = 7.30 and $[Cys]_0 = 100-200$ mM at pH = 7.00 (see the data of Table S2 in Supporting Information).

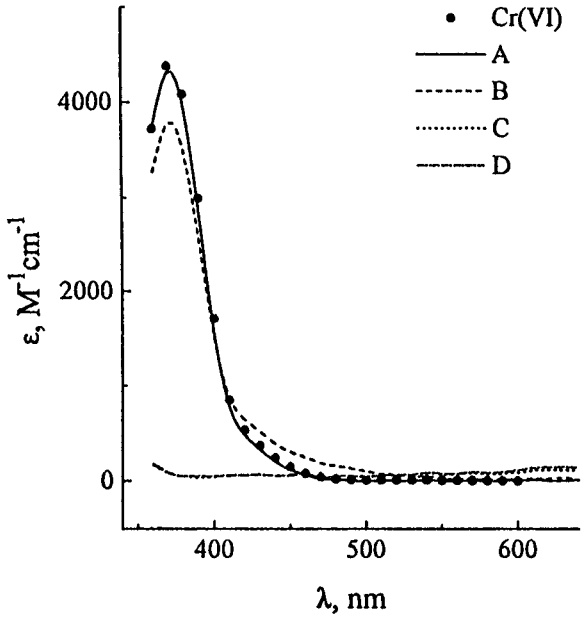

Figure 3. Typical estimated spectra (cubic splines of the global analysis data) for the initial, intermediate, and final species in the reaction Cr(VI) + Cys (conditions I in Table 1): $[Cr(VI)]_0 = 1$ mM; $[Cys]_0 = 200$ mM; $[NaOH]_0 = 20$ mM (pH = 7.30); $[NaClO_4] = 1$ M; 298.1 K. Cr(VI) - control spectrum of $[CrO_4]^{2-}$ (1 mM Na_2CrO_4 + 1 mM NaOH + 1 M $NaClO_4$).

The values of k_i^{obs} are independent of $[Cr(VI)]_0$, thus confirming the validity of pseudo-first-order kinetics (Scheme 3) for the studied process. The dependences of k_i^{obs} on $[Cys]_0$ and pH were studied in terms of the protonated (RSH) and deprotonated (RS^-) forms of substrate (eqs 1 and 2). The following dependences were found:

$$k_1^{obs} = a_1 + b_1[RS^-] \quad (3)$$

$$k_2^{obs} = (a_2[RSH]^2)/(1 + b_2[RSH]) \quad (4)$$

$$k_3^{obs} = a_3 \quad (5)$$

The parameters a_i and b_i for different reaction conditions are enumerated in Table 2. The value of k_1^{obs} increases with increasing ionic strength μ ($[NaClO_4] = 0-0.5$ M), while that of k_2^{obs} decreases with increasing μ and k_3^{obs} is practically independent of μ (see the data of Table S2).

Figure 3 shows typical spectra for species **A**−**D**, estimated from the kinetic data with the use of Scheme 3. The spectra of **A** are consistent with those of $[CrO_4]^{2-}$. The spectra of **B**, which differ from **A** by a slightly decreased extinction at 360−400 nm and a new absorbance band at 410−500 nm, are attributed to intermediates with a high oxidation state of Cr. Finally, the spectra of species **C** and **D** possess weak absorb-

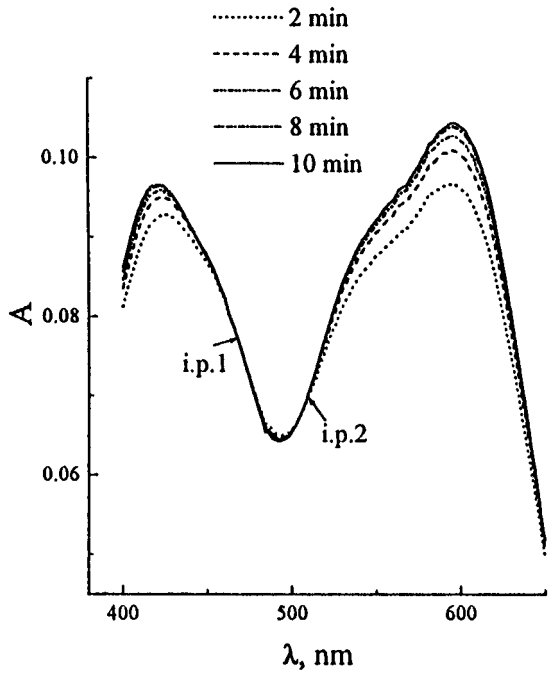

Figure 4. Observed spectral changes under the longer time scale of the Cr(VI) + Cys reaction (diode-array spectrophotometer, $l = 1$ cm; other conditions correspond to Figure 3). Isosbestic points (i.p.) are at 470 and 505 nm.

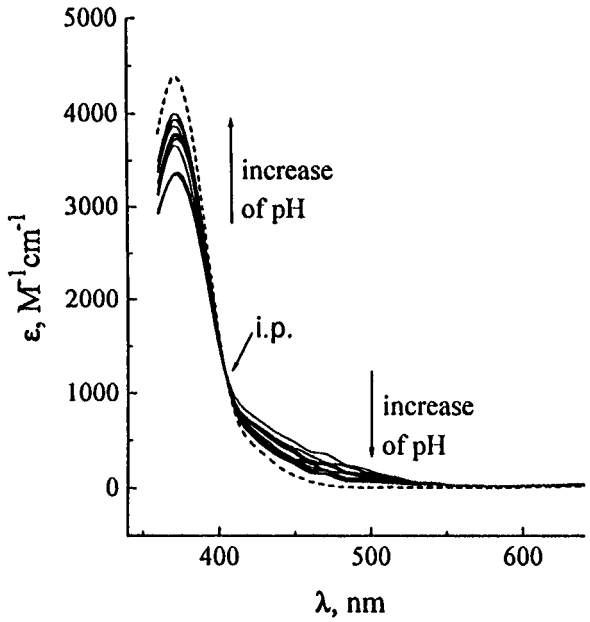

Figure 5. Analysis of estimated spectra of species B (Scheme 3): $[Cr(VI)]_0 = 1$ mM; $[Cys]_0 = 200$ mM; $[NaOH]_0 = 10-40$ mM (pH = 7.0−7.6); $[NaClO_4] = 1$ M; 298.1 K. Changes of estimated **B** spectra with pH (solid lines); estimated spectrum of substance **A** (dashed line; independent of pH). Isosbestic point (i.p.) is at 405 nm.

ances at 400−420 and 550−640 nm, which are characteristic for Cr(III) complexes.[12,13] **D** is distinguished from **C** by increased absorbance at 600−640 nm. However, the absorbances of species **C** and **D** under the studied conditions are too weak to be studied in detail.

The sequential formation of Cr(III) products (corresponding to **C** and **D** in Scheme 3) was observed easily in the experiments with the diode-array spectrophotometer under conditions I (Table 1), but with the increased reaction time and path length (1.0 cm instead of 0.2 cm used in stopped-flow experiments). The time-dependent spectra, shown in Figure 4, were recorded at 2−10 min after mixing of reagents, i.e., after the complete disappearance of Cr(VI). The following features confirm the sequential formation of at least two different Cr(III) species: two isosbestic points at 470 and 505 nm; changes in the ratio of absorbances at 540 and 600 nm; and a shift of absorbance maximum from 425 to 410 nm.

While the estimated spectra of **A**, **C**, and **D** did not change significantly with changing reaction conditions, slight dependences of the spectra of **B** on $[Cr(VI)]_0$, $[Cys]_0$, and pH were observed. The spectra of **B** were most sensitive to the pH value of the solution (Figure 5). The differences between the spectra of **A** (dashed line in Figure 5) and **B** decrease with increasing pH. The changes depicted in Figure 5 show that the spectra of **B** are due to the sum of at least two components: substance **A** and the "red" component **E**, absorbing at 400−500 nm.[22] Taking into account the rate law for the stage **A** → **B** (eq 3), the following equilibrium was ascertained:

$$\mathbf{A} + RS^- \underset{k_{-1}}{\overset{k_1}{\rightleftharpoons}} \mathbf{E} + 2OH^- \qquad (6)$$

where $\mathbf{A} = [CrO_4]^{2-}$ and $K = k_1/k_{-1} = (3.2 \pm 0.7) \times 10^{-13}$ M ($\mu = 1$ M; $T = 298.1$ K).

(22) More detailed studies of the region 360−380 nm (kinetic curves were acquired every 1 nm) did not reveal any shift of absorbance maximum (372 nm) for **B** in comparison with **A**.

Within the experimental error, the value of K and the estimated spectrum of **E** ($\lambda_{max} \sim 430$ nm; $\epsilon_{max} \sim 1600$ M^{-1} cm^{-1}; see Figure S5 in Supporting Information) are independent of pH, $[Cys]_0$, and $[Cr(VI)]_0$. Calculations of K from the data of kinetic experiments are presented in Table S4 (Supporting Information). The stoichiometry of eq 6 is supported by the following experimental observations: (i) the increase of k_1^{obs} with increasing ionic strength (see above) corresponds to the reaction between two negatively charged species; and (ii) the increase in the pH immediately after the mixing of $[CrO_4]^{2-}$ and Cys solutions (see note to Table 1) corresponds to the formation of OH^-. It should be noted, however, that the attempts to include the equilibrium stage to Scheme 3 for global analysis were unsuccessful. The optimized rate constants for the reverse reaction in the eq 6 were extremely low.

Thus, a preliminary assignment of species **A**−**D** (Scheme 3) is clear from their estimated spectra and kinetic behaviors (eqs 3−5): **A** corresponds to $[CrO_4]^{2-}$, **B** is an equilibrium mixture of $[CrO_4]^{2-}$ and substance **E** formed in the reaction between $[CrO_4]^{2-}$ and the deprotonated form of Cys, and **C** and **D** are Cr(III) complexes.

Time-Dependent Spectra Studies (conditions II in Table 1). The main spectral events over the longer time scales of the diode-array measurements are (Figure S6 in Supporting Information) a decay of Cr(VI) absorbance (λ_{max} 280 and 370 nm) and a growth of the intense absorbance with $\lambda_{max} \sim 260$ nm, characteristic for the Cr−S charge transfer band of Cr(III)−Cys complexes.[12,13] The first stage observed by the stopped-flow technique (**A** → **B** in Scheme 3) is too fast to be detected by the present method. Correspondingly, application of SVD to the time-dependent spectra shows the sequential appearance of three components (Figure S7 in Supporting Information). Scheme 4, consisting of two pseudo-first-order processes, can be readily fitted for all kinetic experiments. The optimized $k'_i{}^{obs}$ values for all kinetic experiments are enumerated in Table S5 (Supporting Information). Both $k'_2{}^{obs}$ and $k'_3{}^{obs}$ values are independent of $[Cr(VI)]_0$ and pH. The dependency of $k'_2{}^{obs}$ on $[Cys]_0$ is described by an eq analogous to eq 4, and the resulting parameters are listed in Table 2. The values of $k'_3{}^{obs}$ increase

Scheme 4. Simplest Kinetic Model for the Reaction Cr(VI) + Cys under Conditions II (Table 1)

$$\mathbf{B'} \xrightarrow{k'^{obs}_2} \mathbf{C'} \xrightarrow{k'^{obs}_3} \mathbf{D'}$$

with increasing $[Cys]_0$; however, no mathematical description of this dependency was obvious because of the large scatter in the data.

Typical estimated spectra of the species **B′**−**D′** (Scheme 4) are shown on Figure 6. The spectrum of **B′** is close to that of $[CrO_4]^{2-}$, while the spectrum of **D′** corresponds to the spectrum of the final Cr(III) product, obtained at higher concentrations of reagents (see Figure 1a), and is assigned as being due to $[Cr(Cys)_2]^-$. As was mentioned above, identical rate laws were obtained for processes **B′** → **C′** (Scheme 4) and **B** → **C** (Scheme 3). The estimated spectra of the species **C′** (Figure 6) possess an intense band with $\lambda_{max} \sim 250$ nm,[23] which may be attributed to Cr(III) complex containing a Cr(III)−S bond.[12−13] These observations lead to an assignment of species **B′**, **C′**, and **D′** (Scheme 4, Figure 6) to be identical to species **B**, **C**, and **D** (Scheme 3, Figure 3). Thus, the observed spectral changes for the reaction Cr(VI) + Cys at small initial concentrations of reagents (conditions II in Table 1) are described as the transformation of Cr(VI) to a precursor Cr(III) complex, which is then converted to the final product, $[Cr(Cys)_2]^-$.

The reactions of Cr(VI) with Cys and the related thiols, **4** and **5** (Scheme 2), were studied under identical conditions. The results of global analysis show the close resemblance of the reaction of Cys or **4** with Cr(VI) in terms of both the rate constants (Table 3) and the spectra of the sequentially formed products (Figure S8 in Supporting Information). By contrast, a single product with much less absorbance at 260 nm is formed in the reaction of Cr(VI) with **5** (Figure S8); furthermore, Cr(VI) disappears ∼15 times slower in this case (Table 3).

Additional Kinetic Studies of the Cr(VI) + Cys Reaction. All the previous kinetic results were obtained in Ar-saturated solutions. An attempt was also made to determine the influence of oxygen on the kinetics of the studied processes.[24] However, under conditions I (Table 1), the initial concentrations of O_2 in an air-saturated solution (∼0.25 mM at 25 °C) were much less than the initial concentrations of Cr(VI) (typically 1 mM), but diffusion of aerial oxygen into the reaction mixture during the stopped-flow experiment was negligible. Therefore, no significant effect of aerial oxygen to the reaction kinetics under conditions I was observed. On the other hand, under conditions II (Table 1), when $[O_2]_0 \gg [Cr(VI)]_0$ for air-saturated solutions, the presence of O_2 led to significant autoxidation of Cys to Cys-Cys during the reaction.[25] Thus, we were unable to reveal the specific effect of O_2 on Cr(VI) + Cys reaction kinetics.

Some kinetic experiments under conditions I were performed in the presence of 50 mM Na_2EDTAH_2. No significant effect of this strong chelating agent on the kinetics of the Cr(VI) + Cys process was observed. Thus, the catalysis of the studied reaction by trace metal ions is unlikely.[26]

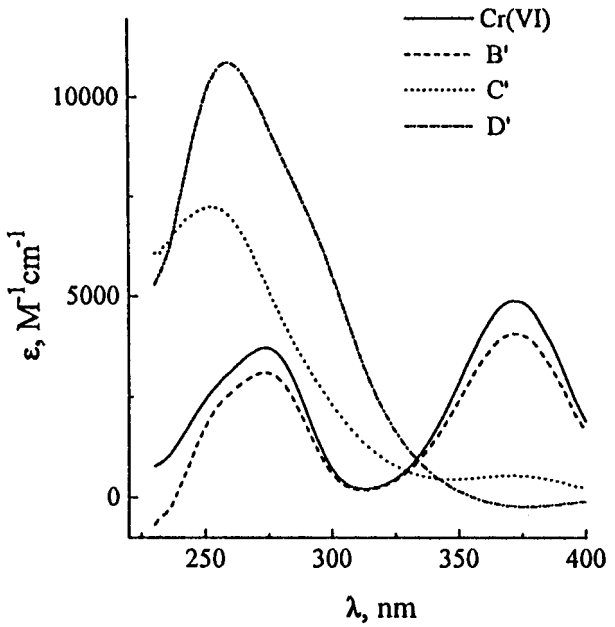

Figure 6. Typical estimated spectra for the reactions of Cr(VI) with Cys (conditions II in Table 1): $[Cr(VI)]_0 = 0.025$ mM; $[thiol]_0 = 4.0$ mM; pH = 7.3; $[NaClO_4] = 0.1$ M; 298.1 K. Cr(VI) - control spectrum of $[CrO_4]^{2-}$ (0.025 mM Na_2CrO_4 + 1 mM NaOH + 0.1 M $NaClO_4$).

Table 3. Observed Rate Constants for the Reactions of Cr(VI) with Different Thiols[a]

thiol	$10^3\, k'^{obs}_2$, s^{-1}	$10^3\, k'^{obs}_3$, s^{-1}
Cys	2.30	0.75
4	2.41	1.29
5	0.192	

[a] Conditions II from Table 1. $[Cr(VI)]_0 = 0.025$ M; $[thiol]_0 = 4.0$ mM; pH = 7.3; $[NaClO_4] = 0.10$ M; $T = 298.1$ K.

Reaction Cr(V) + Cys (conditions I from Table 1).[27] $[CrO(ehba)_2]^-$ is the most convenient source of relatively stable Cr(V).[15] The main features of the reaction between $[CrO(ehba)_2]^-$ and Cys under the studied conditions are (Figure S9 in Supporting Information; the most characteristic kinetic curves at 510, 620, and 640 nm are shown oin Figure 7) as follows: (i) a fast disappearance of the initial absorbance at 360−390 nm (∼0.2 s in comparison with ∼30 s for Cr(VI) under the same conditions); (ii) a fast growth and decay of an intermediate absorbance at 420−590 nm ($\lambda_{max} \sim 510$ nm); (iii) similar, but slower growth and decay of intermediate absorbance at 600−640 nm, ($\lambda_{max} > 640$ nm); and (iv) at 610−630 nm, the fast formation and disappearance of the intermediate followed by a slow increase of product absorbance. UV−visible and CD spectra of the final product are similar but not identical to the corresponding spectra of authentic $[Cr(Cys)_2]^-$ solutions (Figure 1). Thus, at least two intermediates are formed in parallel in the reaction of $[CrO(ehba)_2]^-$ with Cys in neutral medium. Unfortunately, due to the complex nature of the Cr(V) + Cys process under the studied conditions, we are unable as yet to obtain satisfactory global fits of the kinetic data.

(23) For the experiments with $[Cys]_0 \leq 5$ mM (conditions II), the estimated spectra of species **C′** showed some absorbance with $\lambda_{max} = 372$ nm, which indicates the presence of $[CrO_4]^{2-}$ (up to 15% of initial Cr(VI); see Figure 6). It suggests that, at low concentrations of Cys, minor processes leading to regeneration of Cr(VI) (probably the disproportionation of Cr(V) and Cr(IV) intermediates) occur. However, as this phenomenon was not observed at higher $[Cys]_0$, i.e., in the absolute majority of experiments (see Figure 3), it was not further analyzed in the current work.

(24) The influence of O_2 on the reactions of Cr(VI) with thiols, which was presumed to be connected with the formation of oxygen-sensitive Cr(II) intermediates, was recently reported: Perez-Benito, J. F.; Arias, C.; Lamrhari, D. *New J. Chem.* **1994**, *18*, 663−666.

(25) As was shown in separate experiments, such autoxidation did not take place in Ar-saturated solutions.

(26) Bunnett, J. F. In *Investigation of Rates and Mechanisms of Reactions. Part 1*, 4th ed.; Bernasconi, C. F., Ed.; John Wiley & Sons: New York, 1986; p 238.

(27) The stopped-flow equipment was protected from light during the experiments with Cr(V). Under these conditions, decomposition of the initial water solution of $[CrO(ehba)_2]^-$ during the experiments was less than 10% (as determined from the absorbance changes at 510 nm).

Scheme 5. Proposed Mechanism for the Cr(VI) Reaction with Cys in Neutral Media

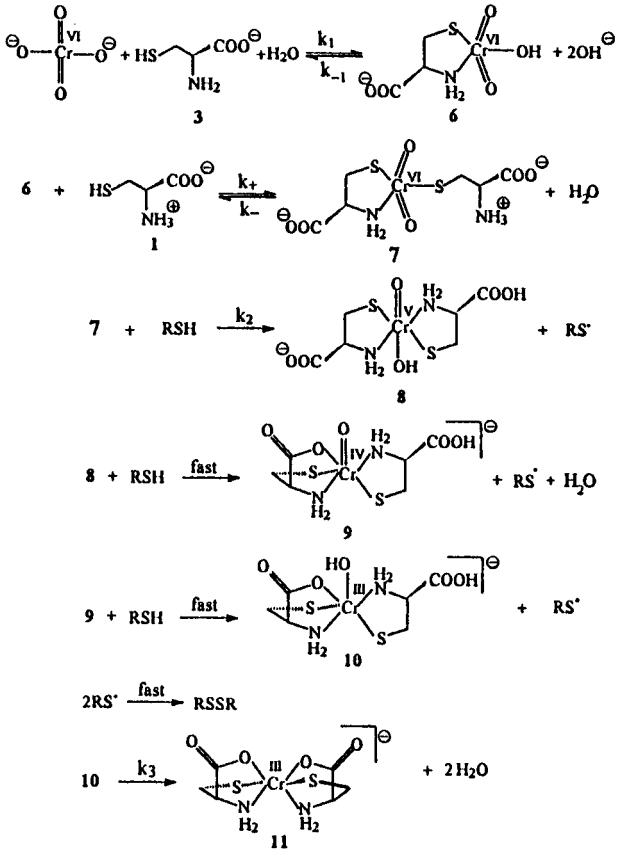

Discussion

The simplest sequence of steps in the Cr(VI) reduction to Cr(III) by Cys in neutral media, consistent with our kinetic and product studies, is presented in Scheme 5.

The first step in the determination of the possible mechanism was the identification of the reaction product. Its UV−visible and CD spectroscopic features, as well as ion-exchange behavior, correspond to those of the crystallographically characterized[11] sodium *N*(*cis*),*O*(*cis*)*S*(*trans*)-bis(L-cysteinato(2−))-chromate(III) (species **D** in Scheme 3, **11** in Scheme 5). This conclusion is in agreement with the results of previous studies[6] of the Cr(VI) + Cys reaction in neutral solutions. Our study showed that complex **11** is formed from the other Cr(III) complex in a relatively slow process (stage **C** → **D** in Scheme 3). The sequential formation of two different Cr(III) complexes in the Cr(VI) + Cys reaction was not observed in previous kinetic studies.[6−8] At high initial concentrations of Cys (conditions I in Table 1), the rate constant of stage **C** → **D** is independent of both $[Cys]_0$ and pH (eq 5). Therefore, complex **11** is formed by intramolecular rearrangement of the precursor Cr(III) complex rather than by addition of a new ligand or a protolytic reaction. A comparison of the Cr(VI) reaction with Cys to those of the related thiols, **4** and **5,** leads to the conclusion that thio and amino groups of Cys are responsible for the formation of the precursor complex (**10** in Scheme 5). Indeed, the rates of formation and UV spectra of the precursor Cr(III) complexes are very similar for the reactions of Cr(VI) with Cys and **4**, and both these features are very different for the reaction of Cr(VI) with **5** (Table 3, Figure S8). Thus, the third spectrally observed stage of the process Cr(VI) + Cys (**C** → **D** in Scheme 3), described by the rate law (eq 5), corresponds to the transformation of a precursor Cr(III) complex, **10,** to the final product **11** (Scheme 5). Reactions of a similar type (intramolecular lactonization at a metal center) are known for Co(III) complexes.[28]

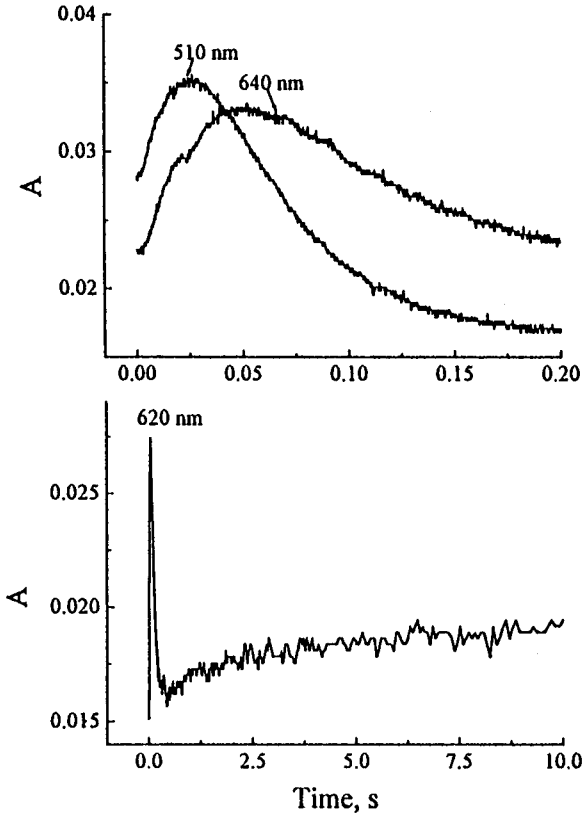

Figure 7. Characteristic kinetic curves for the reaction Cr(V) + Cys (conditions I in Table 1): $[Cr(V)]_0 = 0.7$ mM; $[Cys]_0 = 200$ mM; $[NaOH]_0 = 20$ mM (pH = 7.25); $[NaClO_4] = 1$ M; 298.1 K.

It is generally accepted[29] that the ligand-exchange reactions of Cr(III) complexes are slow (hour time scale at 25 °C). Therefore, the ligand environment of complex **10** should be formed in the previous stages with the participation of labile intermediate complexes in higher oxidation states of Cr. The nature of such intermediates was deduced from the results of experiments with the use of Cr(V) instead of Cr(VI) (Figure 7). The growth and decay of absorbance at ∼510 nm were observed previously by Bose and co-workers[30] for the reactions of $[CrO(ehba)_2]^-$ with organic and inorganic reductants in slightly acidic media. These absorbance changes were attributed to the formation and decay of an intermediate Cr(IV)−ehba complex. On the other hand, O'Brien and Ozolins[31] observed the formation and decay of an intermediate with $\lambda_{max} = 650$ nm during the reaction of Cr(VI) with GSH at pH ∼ 7. This intermediate absorbance was attributed to a Cr(V)−GSH complex, containing a Cr−S bond. From the comparison of the above-mentioned literature data with the data of Figure 7, it is assumed that two main processes occur in parallel during the reaction of the Cr(V)−ehba complex with Cys in neutral medium: (i) reduction of the Cr(V)−ehba complex by Cys via a Cr(IV)−ehba intermediate (corresponding to absorbance changes at 420−590 nm); and (ii) a ligand-exchange reaction with subsequent reduction of Cr(V)−Cys complex, presumably via a Cr(IV)−Cys intermediate (corresponding to absorbance

(28) Boreham, C. J.; Buckingham, D. A.; Francis, D. J.; Sargeson, A. M.; Warner, L. G. *J. Am. Chem. Soc.* **1981**, *103*, 1975−1981.
(29) Cotton, F. A., Wilkinson, G. *Advanced Inorganic Chemistry*, 5th ed.; John Wiley & Sons: New York, 1988; p 687.
(30) (a) Bose, R. N.; Gould, E. S. *Inorg. Chem.* **1985**, *24*, 2832−2835. (b) Ghosh, S. K.; Bose, R. N.; Gould, E. S. *Inorg. Chem.* **1987**, *26*, 3722−3727.
(31) O'Brien, P.; Ozolins, Z. *Inorg. Chim. Acta* **1989**, *161*, 261−266.

changes at 600−640 nm). Applying these data to the Cr(VI) + Cys reaction, the precursor Cr(III) complex **10** is assumed to be formed in two sequential fast one-electron reductions from a Cr(V) complex **8** through a Cr(IV) complex **9** (Scheme 5). The assigned six-coordinate structures of complexes **8** and **9**, with an oxo group and two ligands forming five-membered rings, correspond to the structures of known relatively stable Cr(V) and Cr(IV) complexes.[32−34] However, as the reduction of Cr(V) by Cys is ∼2 orders of magnitude faster than the corresponding reaction between Cr(VI) and Cys under the same conditions, no direct spectral evidence for the formation of Cr(V) and Cr(IV) intermediates during the reaction of Cr(VI) with Cys could be obtained.

The sequence of steps, leading from the initial Cr(VI) compound, $[CrO_4]^{2-}$,[35] to **8**, is proposed on the basis of kinetic data. The rate law (eq 3) for the first spectrally observed stage of the reaction Cr(VI) + Cys (**A** → **B** in Scheme 3) corresponds to a reversible reaction of $[CrO_4]^{2-}$ with RS^- (deprotonated form of Cys).[36] The analysis of the dependences between the reaction conditions and the estimated spectra of **B** (Figure 5) led to the equilibrium, described by eq 6. The maximum concentration of species **E** (eq 6), estimated from the spectral data, decreased from ∼30% $[Cr(VI)]_0$ at pH = 7.0 to ∼10% $[Cr(VI)]_0$ at pH = 7.6. The spectral characteristics of the intermediate **E** (λ_{max} ∼ 430 nm, ϵ_{max} ∼ 1600 M^{-1} cm^{-1}) are similar to those reported by McAuley and Olatunji[37] and Bose *et al*.[38] for the intermediates in reactions of Cr(VI) with thiols in acidic media. In the former work, these spectra were attributed to Cr(VI) thioesters and, in the latter, to Cr(IV) intermediates. However, in acidic media the intermediates were formed in the reaction of $[HCrO_4]^-$ with RSH,[37,38] which disagrees with the rate law found for the reaction in neutral medium (eq 3). Furthermore, the formation of a relatively stable Cr(IV) intermediate in the studied system seems improbable from the results of our experiments on the Cr(V)/Cys system. The formation and decay of the intermediate with λ_{max} ∼ 430 nm in the reaction of Cr(VI) with Cys in neutral medium have been observed by Connett and Wetterhahn,[7] this phenomenon being identified with the formation of thioester $[CrO_3SR]^-$. However, in subsequent works[3,39] these authors have shown that the thiols, including Cys, can form such thioesters only in the reactions with $[Cr_2O_7]^{2-}$ (not $[CrO_4]^{2-}$) at pH < 6.5. Thus, the nature of the reaction between $[CrO_4]^{2-}$ and deprotonated Cys at pH ≥ 7 (eq 6) cannot be explained from the literature data. The likely reason why $[CrO_4]^{2-}$ reacts with RS^- (not RSH) at these higher pH values is that the formation of a Cr(VI)−chelate complex (**6** in Scheme 5) is facilitated by deprotonation of the Cys NH_3^+ group. These results suggest that the first spectrally observed stage of the process Cr(VI) + Cys (**A** → **B** in Scheme 3), described by the rate law (eq 3), is connected with the reversible formation of the Cr(VI) compound, possibly with structure **6** (Scheme 5).

The rate law (eq 4) for the second spectrally observed stage of the process Cr(VI) + Cys (**B** → **C** in Scheme 3) corresponds to the following sequence of reactions:[40]

$$\mathbf{B} + \mathrm{RSH} \underset{k_-}{\overset{k_+}{\rightleftharpoons}} \mathbf{F} \qquad (7)$$

$$\mathbf{F} + \mathrm{RSH} \xrightarrow{k_2} \mathbf{C} \qquad (8)$$

where **F** is the intermediate complex.

The rate laws and the reaction schemes, analogous to eqs 4, and 7, and 8, were used in previous publications[6−8] for a description of the whole process, Cr(VI) + Cys, in neutral media.[41] The literature parameters of eq 4 for different reaction conditions vary over the intervals a_2 = 120−520 M^{-2} s^{-1}; b_2 = 65−600 M^{-1} (Table S6 in Supporting Information).[6−8] These values are in reasonable agreement with those shown in Table 2. The data of Table 2 show a large increase of a_2 and b_2 values with decreasing ionic strength. However, the information available to date is insufficient for the detailed analyses of dependences between a_2 and b_2 values and the reaction conditions.

The obvious question is, do the equilibria, given by eqs 6 and 7, correspond to the same process? If this is the case, the parameters in eq 4 should be dependent on pH. However, a thorough analysis of kinetic data (see note to Table 2) showed that both a_2 and b_2 are independent of pH. Therefore, the equilibria described by eqs 6 and 7 are of a different chemical nature.

If eq 7 is a rapid pre-equilibrium and eq 8 is the rate-determining step, the equilibrium constant will be equivalent to the b_2 parameter (eq 4 and Table 2). If the rapid pre-equilibrium assumption is correct, these large equilibrium constants would lead to practically complete transformation of **B** to an intermediate **F** before significant amounts of **C** are formed (eqs 7 and 8). However, no spectral evidence for such a transformation was obtained. Therefore, the rapid pre-equilibrium assumption is improbable and **F** is assumed to be a steady-state intermediate, which cannot be detected spectroscopically due to its small concentration. This leads to the deduction that eq 7 corresponds to the reversible condensation of complex **6** with a second Cys molecule leading to intermediate **7**, and eq 8 corresponds to the reduction of **7** by the third Cys molecule with the formation of Cr(V) complex **8** (Scheme 5). Thus, the second spectrally observed stage of the process Cr(VI) + Cys (**B** → **C** in Scheme 3), described by the complex rate law (eq 4), corresponds to the multistep transformation of the Cr(VI) complex **6** to the precursor Cr(III) complex **10**. The assumed sequence of steps is represented in Scheme 5.

Correspondingly to Scheme 5, all chemical reactions responsible for the observed spectral changes are of an associative rather than a dissociative nature. This is in agreement with large negative $\Delta S^{\ddagger}$ values, estimated from the temperature dependences of k_i^{obs} (Table S3).

As Scheme 5 shows, 5 mol of Cys are consumed per mole of Cr(VI) in the studied redox process. This corresponds to the overall stoichiometry of the process, established by Kwong and Pennington.[6] It should be noted that Scheme 5 does not contain any reactions between Cr complexes. This is in agreement with the first-order dependence on [Cr(VI)], which is maintained throughout the process (see Results). Such

(32) Mitewa, M.; Bontčhev, R. *Coord. Chem. Rev.* **1985**, *61*, 214−272.
(33) Farrell, R. P.; Lay, P. A. *Comments Inorg. Chem.* **1992**, *13*, 133−175.
(34) Gould, E. S. *Coord. Chem. Rev.* **1994**, *135/136*, 651−684.
(35) The equilibrium concentration of $[HCrO_4]^-$ at pH = 7.0−7.7 is 1−5% of $[Cr(VI)]_0$ (K_a ($HCrO_4^-/CrO_4^{2-}$) = 1.9 × 10^{-6} M^{-1} ($[NaClO_4]$ = 1 M, 298 K): Brasch, N. E. Ph.D. Thesis, University of Otago, 1993. Therefore, $[HCrO_4]^-$ is unlikely to play a significant role in the studied process.
(36) The dependence between the parameters of eq 3 and the rate constants in eq 6 is: $a_1 = k_{-1}$; $b_1 = k_1$: Espenson, J. H. *Chemical Kinetics and Reaction Mechanism*; McGraw-Hill: New York, 1981; p 45.
(37) McAuley, A.; Olatunji, M. A. *Can. J. Chem.* **1977**, *55*, 3328−3334.
(38) Bose, R. N.; Moghaddas, S.; Gelerinter, E. *Inorg. Chem.* **1992,** *31*, 1987−1994.
(39) Brauer, S. L.; Hneihen, A. S.; McBride, J. S.; Wetterhahn, K. E. *Inorg. Chem.* **1996**, *35*, 373−381.
(40) The dependences between the parameters of eq 4 and the rate constants in eqs 7−8 are: (i) if **F** is formed in rapid pre-equilibrium, $a_2 = k_+k_2/k_-$, $b_2 = k_+/k_-$; (ii) if **F** is the steady-state intermediate, $a_2 = k_+k_2/k_-$; $b_2 = k_2/k_-$.[6−8]
(41) In the cited works, it was assumed that [RSH] = $[Cys]_0$.

behavior is likely to be associated with the large $[Cys]_0/[Cr(VI)]_0$ ratios used in this work. A decrease of this ratio will lead to changes in the kinetic features.[23] Generally speaking, Scheme 5 should not be considered as a claim for a universal mechanism of the Cr(VI) reaction with Cys, since it corresponds to the kinetic regularities found in a certain region of reaction conditions (Table 1). Any significant changes of reaction conditions (such as a decrease in the $[Cys]_0/[Cr(VI)]_0$ ratio, major changes in pH, or addition of buffers) will make alternative mechanisms more likely, so new kinetic studies will be required.

The likely changes of Cr(VI) reduction mechanisms with changing Cr(VI)/thiol ratio should also be taken into account when the role of these reductions in Cr(VI) genotoxicity is discussed. Thus, the formation of relatively stable Cr(V)−thiol complexes in Cr(VI) reactions with Cys and GSH (Cr(VI)/thiol = 1/1−1/20) in neutral aqueous media has been detected by EPR spectroscopy.[4,42] Such complexes were assigned as one of the possible active species leading to the Cr(VI)-associated DNA damage.[2] However, the present work does not give any evidence for the formation of stable Cr(V) or Cr(IV) intermediates in the reduction of Cr(VI) by a large (at least 50-fold) excess of Cys. As the rate of intracellular reduction of Cr(VI) is probably determined by Cr(VI) diffusion through the cell membrane,[43] the *in vitro* mechanistic studies of Cr(VI) reductions are likely to be more biologically relevant when carried out in the presence of reductant in great excess, not in near-stoichiometric conditions. Therefore, the kinetic results reported here suggest that the complexes of biological thiols (Cys and GSH)[44] with the intermediate oxidation states of Cr are unlikely to take a significant part in Cr(VI)-caused genotoxicities.[45]

Acknowledgment. The support of this work by Australian Research Council (ARC) grant (to P.A.L.) and by an ARC infrastructure grant for purchase of stopped-flow and CD instruments is gratefully acknowledged. The authors thank Assoc. Prof. Surendra Mahapatro (Regis University, Denver, CO) for helpful discussions.

Supporting Information Available: Tables and figures presenting the details of kinetic analyses: initial kinetic data in coordinates of absorbance−wavelength−time; characteristic kinetic curves; results of SVD; optimized rate constants; activation parameters; and estimated spectra of intermediates (16 pages). Ordering information is given on any current masthead page.

IC960663A

(42) Kitagawa, S.; Seki, H; Kametani, F.; Sakurai H. *Inorg. Chim. Acta* **1988**, *152*, 251−255.

(43) Dillon, C. Ph.D. Thesis. University of Sydney, 1995.

(44) Although GSH is generally considered to stabilize the intermediate redox states of Cr more efficiently than Cys,[4,31,38,42] the Cr(V)/GSH and Cr(IV)/GSH complexes are likely to be reduced rapidly by a great excess of GSH (up to 8 mM),[1] present in intracellular media.

(45) This hypothesis is supported by the recent observation that the isolated Cr(V)/GSH complex, unless activated by molecular oxygen, does not cause single-strand breaks in isolated DNA: Kortenkamp, A.; Casadevall, M.; Faux, S. P.; Jenner, A.; Shayer, R. O. J.; Woodbridge, N.; O'Brien, P. *Arch. Biochem. Biophys.* **1996**, *329*, 199−207.